12-2013

Feasibility of using computational fluid dynamics for analysis of flow in an orbiting dish.

Matthew R. Purcell
University of Louisville

FEASIBILITY OF USING COMPUTATIONAL FLUID DYNAMICS FOR ANALYSIS OF FLOW IN AN ORBITING DISH

By
Matthew R Purcell
B.S., University of Louisville, 2005

A Thesis
Submitted to the Faculty of the
University of Louisville
in Partial Fulfillment of the Requirements
for the Professional Degree

MASTER OF ENGINEERING

Department of Chemical Engineering

December 2013

FEASIBILITY OF USING COMPUTATIONAL FLUID DYNAMICS
FOR ANALYSIS OF FLOW IN AN ORBITING DISH

Submitted by:_____
Matthew R. Purcell

A Thesis Approved On

_____
(Date)

by the Following Reading and Examination Committee:

_____
Dr. R. Eric Berson, Thesis Director

_____
Dr. M. Keith Sharp

_____
Dr. Gerold Willing

ACKNOWLEDGMENTS

I would like to immensely thank Dr. Berson for his patience and guidance.

Many thanks to Dr. Willing and Dr. Sharp for their reviews and willingness to help with completing this process.

To my loving wife Allison, whose doggedness and persistence has brought me to this finished product. You are the best person I have ever known.

ABSTRACT

The oscillatory flow provided by an orbital shaker table correlates somewhat to the pulsatile flow seen in the human vasculature. This parallel allows for the use of the orbital shaker table in a large range of biomedical research. However, the fluid dynamics is not well characterized in this system.

This research employed the computational fluid dynamics (CFD) package FLUENT in an effort to better understand the fluid dynamics in an orbiting dish. This work was performed at low resolution as a first attempt to examine the fluid flow characteristics. The first objective was to determine the time required to reach a steady state. This was found to occur within four orbits of the dish.

The shear stress on the bottom surface of an orbital dish was then investigated and compared to previously published scalar functions. An equation used in two cases by Ley et al. (1989) determined shear to be 2.76 dyne/cm^2 and 3.12 dyne/cm^2 respectively. These systems had Stokes Numbers of 2 and 2.5, Froude Numbers of 0.7 and 0.8 and Slope Ratios of 0.4 and 0.3 respectively. . When modeled in FLUENT the cases showed the magnitude of shear stress in the center of the dish to be 0.67 dyne/cm^2 and 1.11 dyne/cm^2 respectively. The average shear stress on the bottom of the dish for the same cases was determined to be 0.39 dyne/cm^2 and 0.85 dyne/cm^2 respectively. More revealing, the shear was found to be uneven across the bottom of the dish with maximum shear near the peak of the fluid wave.

Next, cases were simulated across ranges of dimensionless Stokes Number, Froude Number, and slope ratio at low resolution to determine the feasibility of using

FLUENT to observe transitions. Each case was run at a constant Reynolds Number of 100 to maintain laminar flow. A Stokes number transition is evidenced by a lag in the location of the fluid peak relative to the location of the dish. When a gap in the leading edge of the fluid is observed, a Froude number transition has occurred. A large free surface slope resulting in a dry area forming on the bottom of the dish is indicative of a Slope Ratio transition. These transitions were positively identified at low resolution when changing one dimensionless number while keeping the others constant.

TABLE OF CONTENTS

NOMENCLATURE

a = cylinder radius
f = frequency of rotation
Fr = Froude number
F = body force
g = gravitational acceleration
H = mean fluid height
p = pressure
R = orbital radius
Re = Reynolds number
SR = slope ratio
S_m = source term for the addition of mass
St = Stokes number
u = velocity
x = length
y = height
z = depth
ρ = fluid density
τ = shear stress
τ_w = wall shear stress
μ = fluid viscosity
ν = kinematic viscosity
ω = angular velocity

LIST OF TABLES

LIST OF FIGURES

I. INTRODUCTION

The human vasculature is subjected to hemodynamic forces, e.g. blood pressure and cyclic stress. Research on the effects of these forces on the walls of the blood vessels has been done for over thirty years. Even after three decades of research, the mechanisms by which hemodynamic forces affect the vascular system are relatively unknown.

Blood flows through the vasculature in a pulsatile motion, creating a shear stress along the vessel walls, thus affecting endothelial cells both morphologically and physiologically. Studies have shown that this shear stress may promote atherosclerosis, a leading cause of death in the United States. Determining the effect of shear on cells has been widely researched, and many different methods have been employed. While devices such as the cone-and-plate shearing instrument and flow chambers have been used to apply shear stress to cells, they come with limitations. The cone-and-plate device is incapable of producing rapidly changing flow, due to the inertial of the cone. Both have limitations in the number of cases that can be tested simultaneously.

The orbital shaker table is an easy to use instrument that provides oscillatory flow for a cell culture medium. This oscillatory flow somewhat resembles pulsatile flow in the vascular system. Unfortunately, determining shear stress and its effect on cells has been a challenge, since the fluid undergoes a complex flow pattern within a dish on an orbital shaker table. This complexity has led researchers using the orbital shaker table to study cellular response to shear stresses to use over-simplified equations to estimate the wall

shear stress. The orbital shaker is a tool widely used in the field of cell culture study. Its greatest benefit to the research sector is its versatility: a wide variety of experiments may be simultaneously run on the orbital shaker.

This research focuses on employing computational fluid dynamics (CFD) to determine wall shear stress on the bottom surface of the cell culture dish when exposed to conditions created by the orbital shaker table. The software package is able to fully mimic the geometry and motion of the orbiting dish, while using the same fluid properties (e.g., density and viscosity) as those used in culture dishes. By using CFD, shear stress values previously obtained in literature may either be validated or questioned. Since an unsteady state solution was used, one objective was to determine how long each case must be run before the fluid motion reaches steady state.

An important aspect of employing CFD software to resolve the flow in an orbiting dish is that it allows both spatial and temporal dependence to be visualized inside the dish, which other current estimation techniques are incapable of. One widely used estimate by Ley et al. (1989) provides a simplified scalar function to estimate wall shear stress at the bottom of an orbital shaker table dish. Ley's equation just provides a single value for the whole surface, and is limited in that it does not account for the fluid height, a potentially important variable in calculating shear stress. A second objective in this work was to compare CFD results to the estimate presented by Ley et al. for the actual flow conditions in their experiments.

Dimensionless parameters allow one to reduce the number of variables required to define a complete set of flow conditions. Of interest in this research is the fluid behavior at ranges of dimensionless parameters commonly used in cell culture experiments.

Parameters of interest here are the Stokes number, Froude number, and slope ratio. A third objective was to determine the feasibility of identifying transitions in flow characteristics with variations in each of these parameters, while maintaining constant values for the other parameters, using CFD. Determining these transitions involves simulating a series of cases, at a low resolution as a first attempt, until a phase contour shows definitively that a transition occurs. Running these cases at a low resolution will provide a basis from which higher resolution cases may be run. For the Stokes number, a transition occurs when the wave's peak becomes out of phase with the location of the dish in its orbit, while a steep slope at the leading edge of the wave indicates a Froude number transition. A transition occurs for the slope ratio when the observed fluid's wave is sloped enough to create a dry area on the bottom of the dish. The results are useful quantities for describing the regimes of oscillatory flow that can occur in an orbiting dish.

II. LITERATURE REVIEW

A. Effects of Hemodynamic Forces

1. Cellular Responses to Shear Stress

The component of fluid stress at a point tangential to the plane on which the stress acts is known as shear stress (Schaffer et al., 2002). Shear stress is exerted on cells and vessel walls as blood flows through the vascular system. The shear stress that is exerted creates both morphological and biochemical changes in the cells. Levesque and Nerem (1985) showed that high shear stress will cause vascular endothelial cells to be elongated and ellipsoidal in shape while at low shear stresses these cells are more compact and trapezoidal. On a study of rabbits' responses to altered hemodynamics (forces involved in the circulation of blood), Greenhill and Stehbens (1983) found that hemodynamic changes can tear the arterial walls and bring about cardiac arrest and death.

Altering shear stress significantly influences the rate of formation of pinocytotic (ingestion of fluid by the cells) vesicles. This alteration can lead to permanent elevation in pinocytotic rate in the endothelial cells, completely independent of growth stimulation. This process is dependent on time and the amount of force being applied (Davies et al., 1984).

2. Shear Stress and Atherosclerosis

Artherosclerosis, one type of which is coronary artery disease, occurs over time as fatty deposits build up on the arterial walls in the vascular system. This disease is the leading cause of death in developed countries (Malek et al., 1999). Formation of this

disease is a complex process with both local and systemic factors at play (Gotlieb et al., 2001). Zarins et al. (1983) found that flow-induced shear stress plays an important role in plaque localization and grown in the endothelial cells. As aforementioned, shear stress is a strong promoter of the morphological and biochemical response of endothelial cells. Along the walls of the blood vessels, the hemodynamic shear stress is higher than in the inner areas of the vessels. These altered hemodynamics around the curvatures of arteries can lead to the development of complicated plaques associated with atherosclerosis (Resnick et al. 2003). Some studies have shown that when these cells experience low values of shear stress (<4 dyne/cm^2), atherosclerosis is more prone to being developed (Malek et al., 1999) (Alshihabi et al., 1996). Additional studies by Ku (1997) show that shear as a result of oscillatory flow is more crucial to the development of atherosclerosis than the magnitude of the shear. Cunningham et al. (2005) confirmed that vascular endothelium had different behavioral responses to disturbed and oscillatory flow and these responses (i.e. shear stress) play a key role in promoting atherosclerosis.

Shear stress has also been studied after operations to prevent oncoming artherosclerosis (i.e., balloon angioplasty). These results, conducted by Wentzel et al. (2003), show that post-operative shear stresses alter the morphology of the endothelial cells in a similar manner to those stresses observed in cells with no signs of artherosclerosis.

B. Methods to Determine Cell Response to Shear Stress

1. Flow Apparatuses

The ability to determine shear stress within certain accuracies is crucial to the study of shear and its effect on cells. There are a number of apparatuses that are being employed, all of which involve the growth of cells in a cultured environment. One device is a flow chamber in which fluid flows between two parallel plates. With a given rate of fluid flow and distance between the plates, calculating the shear stress on the wall is quite simple. Frangos et al. (1988) employed the flow chamber in studying steady shear stress rates on human umbilical vein endothelial cells. They were able to easily determine the shear due to the steady flow. Unfortunately, these steady results are atypical of the pulsatile flow in the vasculature.

A second type of flow apparatus is the cone-and-plate device, which typically involves rotation of a cone over a monolayer of cells grown on a stationary plate. Ley et al. (1989) investigated shear-dependent adhesion of human granulocytes to endothelial cells using the cone-and-plate device. Similar to the flow chamber, using the cone-and-plate device allows for the wall shear stress to be easily obtained, provided the cone's rotation rate and the distance between the cone and the stationary wall is known. Ley et al. were able to calculate shear for the cone-and-plate experiment.

The common limitation for the flow chamber and cone-and-plate device is that these devices are highly specific, allowing for only one experiment per apparatus to be run at a time. If multiple experiments need to be run, a great deal of time must be expended in performing one test at a time or a large amount of money must be spent to obtain multiple devices.

Another apparatus for providing fluid motion to cultured cells is the orbital shaker platform. Whereas the flow chamber and cone-and-plate device are limited to running

one experiment at a time, orbital shakers allow for multiple samples to be run simultaneously. Their operation is also very simple. Samples cultured in dishes are placed on the shaker table and the table provides an orbiting motion. The oscillatory flow in the shaker table is somewhat related to the pulsatile flow experienced in the vasculature. While the operation of the shaker table is much easier than the flow chamber and cone-and-plate device, calculation of the wall shear stress is much more complex. The difficulties lie in the oscillatory fluid flow because the peak of the wave created will move as the dish orbits, creating oscillating rather than steady shear values. This implies that the actual location of the maximum wall shear stress will move with the rotation of the dish.

2. Simplified Equations

Many researchers have employed simplified equations in order to estimate maximum wall shear stress in the orbiting dish. Along with the previous cone-and-plate experiment mentioned, Ley et al. (1989) performed the same study of granulocytes' adhesion to endothelial cells in an orbital shaker table. The shear stress values obtained by Ley et al. in the orbital shaker table experiments were an estimate of the maximum wall shear stress at the bottom of the cylinder.

$$\tau_w = \sqrt{a \cdot (\rho \cdot \pi \cdot f)^3} \qquad (1)$$

The equation employed does not take into account the fluid height, typically a key piece of information in calculating shear and one that is used when calculating shear for both the flow chamber and cone-and-plate device. There was no explanation by the investigators as to the basis for the equation. Berson, et al. (2006) later showed that the equation corresponds to the magnitude of wall shear stress in the extension of Stokes

second problem to orbital flow. This solution applies for low Reynolds number, low slope parameter, low Froude number and high Stokes number. The Reynolds Number is the ratio of inertial forces to viscous forces (Bird et al., 2002).

$$\mathrm{Re} = \frac{\omega R^2}{\nu} \tag{2}$$

In studying the transitions of dimensionless parameters a low Reynolds number (100) is assumed.

The slope ratio represents the ratio of the slope of the steady state free surface and the aspect ratio of the dish.

$$SR = \frac{R\omega^2}{g} \cdot \frac{a}{H} \tag{3}$$

A transition in flow character is thus expected in an orbiting dish as the slope ratio increases, since a slope ratio of greater than one corresponds to a free surface that intersects the bottom of the dish.

The Froude number can be interpreted as the ratio of the inertial to gravity forces in a flow field (Bird et al., 2002).

$$Fr = \frac{a\omega^2}{g \cdot H} \tag{4}$$

This ratio may also be interpreted physically as the ratio between the mean flow velocity and the speed of an elementary gravity (surface or disturbance) wave traveling over the water surface (McCabe et al., 2001). For the orbiting dish the Froude number correlates to the gradient of the leading edge.

The Stokes number is a dimensionless number representing the ratio of fluid inertial forces to viscous forces.

$$St = H \cdot (\frac{\omega}{\nu})^{1/2} \quad (5)$$

Haga et al. (2003) used the simplified shear equation originated by Ley et al. (1989) when studying the growth of smooth muscle cells in an orbiting shaker table and how oscillatory shear stress affects them. They obtained unexpected results in that smooth muscle cells increased proliferation in response to oscillatory shear stress. Contrary to Haga et al. finding that shear stress due to oscillatory flow increased smooth muscle cell growth, Sterpetti et al. (1993) reported that steady shear stress actually inhibited cell growth. Haga et al. ascribed that oscillatory flow is a better approximation to flow in the vasculature, and therefore their model would be more applicable than Sterpetti et al., who experimented only with steady flows.

The shear equation used by Ley et al. (1989) was also applied by Kraiss et al. (2003) in studying E-selectin protein production and the mechanisms that are limited by fluid flow and that activate p70/p85 S6 kinase in endothelial cells. Employing the simplified shear equation may be a reasonable first estimate as to the maximum shear, but in order to properly quantify the shear stress values on the bottom surface of the orbiting dish, a more precise model needs to be investigated.

Measurements of wall shear stress of an orbiting dish were performed by Dardik et al. (2005). They used optical velocimetry to obtain shear values for proliferating endothelial cells exposed to oscillatory flow on a shaker table. The dish measured 3.5 cm in diameter with a height of 1.8 cm. The fluid under study had a viscosity of 0.0101 poise, density of 0.9973 g/mL, and average particle size of 7 microns. Once the dish was placed inside the shaker, fluid was filled to a height of 0.208 cm and the dish rotated at

210 revolutions per minute about a radius of 0.95 cm. Shear values found at the bottom of the dish near the center were about 5 dyne/cm^2. Shear stress values on the bottom of the dish near the side walls were found to be about 11 dyne/cm^2.

C. Computational Fluid Dynamics (CFD)

1. FLUENT Modeling Processes

FLUENT is a commercial CFD program that allows the user to model fluid flows (i.e. velocity field strength, phase boundaries, and shear stress magnitude). By employing the finite-volume discretization process, FLUENT numerically solves the governing equations for conservation of mass and momentum. In its most basic form, the conservation of mass is shown by the equation:

$$\frac{\partial \rho}{\partial t} + \frac{\partial}{\partial x_i}(\rho u_i) = S_m \tag{6}$$

The equation for conservation of momentum is:

$$\frac{\partial \nu}{\partial t} + \nu \bullet \nabla \nu = -\nabla p + \nabla \bullet \tau + F \tag{7}$$

Shear stress in the conversation of momentum equation is designated by τ_{ij}. This shear component is mathematically represented by the equation:

$$\tau_{ij} = \left[\mu \left(\frac{\partial u_i}{\partial x_j} + \frac{\partial u_j}{\partial x_i} \right) \right] - \frac{2}{3} \mu \frac{\partial u_i}{\partial x_i} \delta_{ij} \tag{8}$$

Substituting the shear component into the conversation of momentum yields the Navier Stokes equation for a Newtonian fluid (with gravity being assumed for body force F):

$$\rho\left(\frac{\partial \nu}{\partial t} + \nu \bullet \nabla \nu\right) = -\nabla p + \nabla \bullet (\mu(\nabla \nu + (\nabla \nu)^T) + \nabla\left(-\frac{2}{3}\mu \nabla \bullet \nu\right) + \rho g \tag{9}$$

FLUENT integrates over the computational grid of cells, reducing the equations to the simplified form (Fluent Inc., 2002):

$$\phi_p \sum_i (A_i - S_P) = \sum_i A_i \phi_i + S_c \tag{10}$$

Contributions from diffusive and convective fluxes are incorporated in the A_i term, while S_p and S_c make up a linear source term:

$$S_\phi = S_c + S_P \phi_P \tag{11}$$

Derivatives of the flow variables are calculated using the power law. This allows FLUENT to interpolate between points on the computational grid.

Using a given set of initial conditions, FLUENT solves the various equations in an iterative fashion. FLUENT will cease iterating when a defined number of iterations are completed, or a given residual value is obtained between iterative solutions (Fluent Inc., 2002).

Before FLUENT is able to analyze flow systems, a pre-processing package must be used. GAMBIT is the main pre-processing software for FLUENT. In GAMBIT, a geometric depiction of the fluid flow region is created. For an orbiting dish a relatively simple cylindrical geometry is created. The total mesh size created in GAMBIT is a determining factor as to how accurate the solution obtained in FLUENT will be. This variable also determines how long the FLUENT solver will run; low mesh counts will take much less time to run than large mesh counts. A cell count of 15000-20000 was used for this research.

Modeling time-dependent or steady state systems is accomplished through the FLUENT solver, which is of interest when looking at orbiting dishes. FLUENT has the

capability of modeling in two or three dimensions under both laminar and turbulent flow. (Fluent Inc., 2002).

In order to properly model the orbiting dish, the mesh must be able to spatially move over time. This is accomplished by importing a user-defined function, a program written in C programming language, which specifies the orbital frequency, radius of orbit, and center of orbit. The air-liquid interface is of importance due to the fluid splashing around inside of the dish. Tracking the surface between the air and the liquid is accomplished using the Volume of Fluid (VOF) model. In the VOF model, the two fluids being modeled share a single set of governing equations and the volume fraction of each fluid in each computational cell is tracked throughout the mesh (Fluent Inc., 2002).

2. CFD as a Research Tool

Modeling programs such as FLUENT that solve the Navier-Stokes equations for pulsatile flow provide a way to predict properties that are otherwise difficult to determine. The number of researchers employing CFD to model the vascular system is increasing tremendously due to the economic feasibility of purchasing the software and the high performance computing capabilities that accompany CFD. It provides the researcher with the ability to visualize certain flow patterns and properties while saving valuable time and money on laboratory experimentation.

III. EXPERIMENTAL

A. Purpose of Investigation

It is the purpose of this investigation to employ FLUENT to determine the motion of fluid in a dish residing on an orbital shaking apparatus, with a particular focus on the wall shear stress on the bottom of the dish. Results will allow for a comparison to be made with calculated shear stress values found in literature from Ley et al. (1989). The process of running FLUENT is much more cost efficient than performing benchtop experiments. FLUENT also has the ability to simulate fluid flow that would be extremely challenging to show in a lab setting. This makes FLUENT an attractive method of solving these cases.

The transitions of the Stokes number, Froude number, and slope ratio all at a constant Reynolds Number are investigated for the case of oscillatory flow using FLUENT. With a Stokes number transition, a lag in the fluid wave is noticed. For a Froude number transition, a discontinuity is found on the leading edge of the fluid wave. A slope ratio transition is noticed when the slope is of great enough magnitude that a bare spot is seen on the bottom surface of the cylinder.

B. Plan of Experimentation

In order to study shear stress on an orbital dish, the commercial CFD package FLUENT will be used. First, a model was created using the geometric modeling program GAMBIT. Through trial and error, a certain number of computational cells were found

that provide an adequate initial estimate of wall shear stress on the bottom of the dish. A cell count too high resulted in long processing times while a cell count too low produced inaccurate results.

Once the proper model was developed, several different cases were investigated to determine shear stress on the bottom wall of the orbiting cylinder. The work done by Ley et al. (1989) was investigated, with a full replication of their fluid properties and dish dimensions using FLUENT. The results of these cases were compared to the estimated value Ley obtained using a simplified wall shear stress equation.

Of more academic interest, several cases were run at varying Stokes numbers, Froude numbers, and slope ratios. By monitoring the wave patterns for each of these values, transition zones were noticed for each. All of these data were run at a relatively low cell count (15,000-20,000 cells) to provide initial estimates of shear and dimensionless transition values, and at constant low Reynolds numbers to maintain laminar flow.

C. Equipment and Materials

Running FLUENT requires a computer with a large amount of processing capacity. For this investigation, a 64 bit Linux cluster parallel system based on the AMD Opteron processor is utilized. The system consists of six nodes with a total of 12 processors, 24 gigabytes of memory, and 2.2 terabytes of disk storage. This system runs both FLUENT Version 6.2.5 and its geometrical modeling software GAMBIT Version 2.3.16.

D. Procedure

1. Creating Orbital Dish Geometry

1. Open GAMBIT, the software used to model flow geometries to import into FLUENT.
2. Create a cylindrical volume, the diameter of which was specified by the value of the respective dimensionless parameters under study (all case parameters are found in Appendix A). The cylinder has the lowest possible height (without the fluid hitting the top) in order to keep the modeled fluid contained within the cylinder so that FLUENT can properly solve the model. This height was found via trial and error. A greater height will result in a lengthier processing time in FLUENT.
3. In order for FLUENT to solve using the finite difference method, a computational mesh was created across the cylinder using the GAMBIT modeler. In order to study cases at a low resolution, a mesh count of 15,000-20,000 cells was used for each case. The results of these cases allowed for an initial determination of dimensionless number transitions.
4. To obtain a mesh count of 15,000-20,000 cells, the Mesh command was initialized. Once this was done the edge of the cylinder was meshed followed by the face and the volume.
5. Under the Mesh Edges toolbar, the base of the cylinder was selected. In the Spacing tab, there are two options: Interval Size and Interval Count. Altering the interval count produced the desired number of computational cells. Initially, an interval count value was input and the edge meshed. If the total cell count was

not within the desired range the process was undone until an interval count was selected that produced the specified number of computational cells.

6. Once an interval count was chosen and the edge meshed, the face was meshed (accessed via the Mesh Faces command). The curved section of the cylinder was selected as the face to be meshed. A projected number of intervals were obtained from a ratio of the cylinder height and diameter.
7. After meshing the face, the total cylinder volume was meshed. This was done by accessing the Mesh Volume command, selecting the entire cylinder, and meshing this volume. The text box at the bottom of the GAMBIT window output a total cell count. This number was compared to the specified range of 15,000-20,000 cells. If the value was out of range then the process was restarted until 15,000-20,000 cells were obtained.
8. Once the range was achieved the mesh was saved as a .msh file and was ready to be imported into FLUENT.

2. Setting up FLUENT Cases

1. With the FLUENT software open, Read Case was selected and the desired .msh file was imported.
2. A Grid Check was performed to ensure that no negative volumes were present.
3. The Smooth and Swap tool was used on the grid nodes to achieve minimum cell skewness until the number of nodes swapped remains constant.
4. The grid scale was converted from meters (the default units of GAMBIT geometries) to centimeters. Under the Scale Grid command the units were altered to “cm” and scaled.

5. An unsteady state solver was activated so that the fluid flow was properly modeled. This was done by accessing the Solver command under the Models window, then selecting "Unsteady" as the option in the Time window.
6. For the cylinder, any fluid region not containing water contained air. Therefore, a multiphase operation was specified. The multiphase modifications were found in the Multiphase Model command window (refer to Figure 1). In this window, the "Volume of Fluid" option was selected.

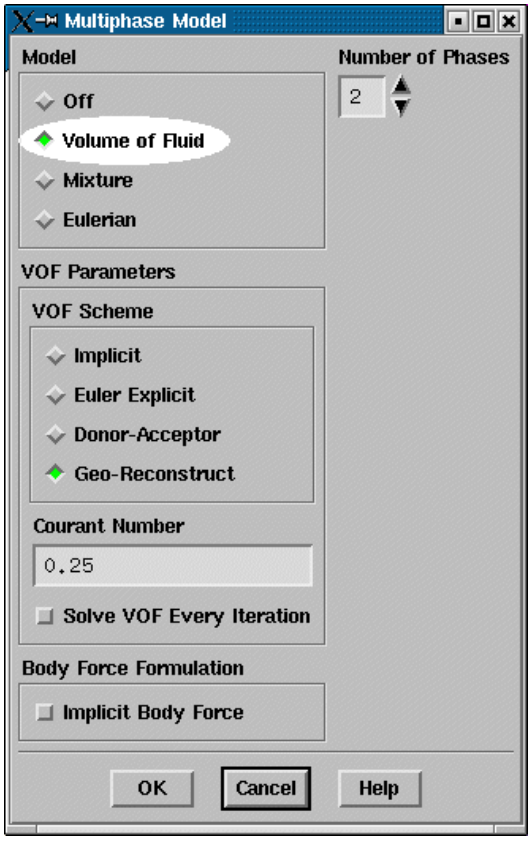

FIGURE 1 – Multiphase Model Window

7. Once the multiphase model was selected the fluids were defined. Under the Define materials window, the "Fluids Database" was searched for liquid water (FLUENT has the fluid preset as "water-liquid"). The properties for the liquid

water were copied and the database was closed. This step was also completed for air.

8. With the fluids defined, the fluid regions were defined. The Define Phases command opened the Phases window. The "Upper (primary phase) Fluid Phase" was set as air and the "Lower (secondary phase) Fluid Phase" was set as the liquid water created in the Materials menu. After each phase was set they were named "air" and "water" respectively.
9. A reference pressure location was selected so FLUENT can properly solve each case. The Operating Conditions window was accessed under the Define tab and an empty text box labeled "Reference Pressure Location" was shown. A value 0.1 cm below the top of the cylinder in the vertical (z) direction was entered (e.g. for a cylinder measuring 2.0 cm high the reference pressure location was set as 1.9 cm).
10. The "Gravity" option was selected in the Operating Conditions window which made the value of gravitational acceleration equal to -9.81 m/s^2 in the vertical (z) direction due to the fact that gravity was acting downward on the fluid.
11. In order to simulate the orbital motion of the cylinder, a User-Defined Function (UDF) was created and compiled into FLUENT (sample in Appendix B). The "orbital speed", denoted by ω (radians/second), was altered in the UDF depending on which case was being run (Appendix A details orbital speed values for each case).
12. Compiling the UDF into FLUENT was done by opening the "Compiled UDF" window, which is a subsection of the Functions command.

13. Once the desired UDF was found, it was placed in a library. Each library name was named starting with mdmlib_ and ending with a title that best represented the case (e.g. mdmlib_CaseA for Case A).
14. With the library properly named, it was then Built and Loaded, insuring that the library was located in the same directory from which FLUENT was running. The library allowed FLUENT to generate mesh motion, also referred to as dynamic mesh.
15. A dynamic mesh was activated under the Dynamic Mesh Parameters menu. In order for FLUENT to read both the fluid and the cylinder, the "Dynamic Mesh Zone" command was implemented. The cylinder wall was selected in the "Zone Names" window motion was selected in the Motion UDF/Profile box.
16. The "Zone Names" procedure was repeated for the fluid.
17. The initial fluid region was then patched to the cylinder volume so that FLUENT recognized both air and water in the cylinder. Before this region was created initialization of the solver was done by selecting the "Init" command in the Solution Initialization menu.
18. As seen in Figure 2 below, the fluid was then patched to the region via the Region Adaptation command. The command brought up a window of coordinates for the minimum and maximum x,y, and z coordinates. The minimum x and y values were the negative radius value of the cylinder, while the maximum x and y values were the positive radius values. On the z coordinate, the minimum was zero and the maximum was the initial fluid height. These coordinates were then marked and the fluid region was ready to be patched.

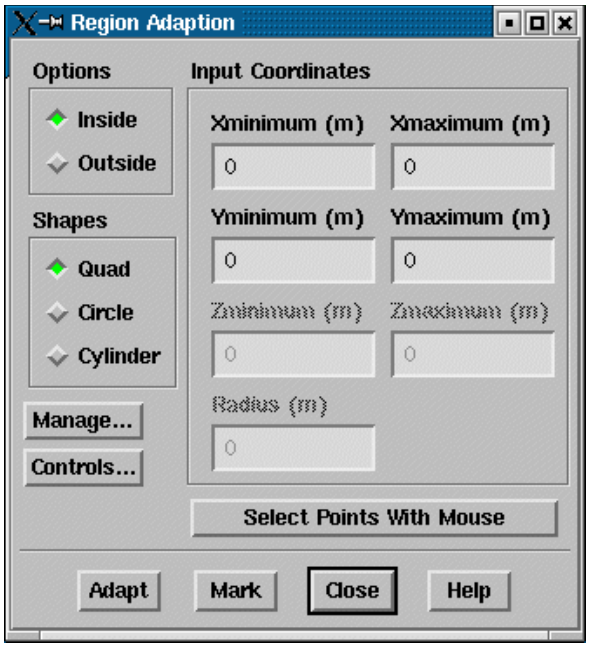

FIGURE 2- Region Adaptation Window

19. The Patch command under the Initialize window was used. When the Phase command appeared "water" was chosen as Type One. In the Registers box "hexahedron-r0" was selected in and the fluid was successfully patched to the cylinder.
20. The Solution Controls menu (see Figure 3) contained the many variables for solving that FLUENT employed. The "Under-Relaxation Factors" were set to 0.3, "Pressure Discretization" to Body Force Weighted, "Momentum Discretization" to QUICK, and "Pressure-Velocity Coupling" to PISO.

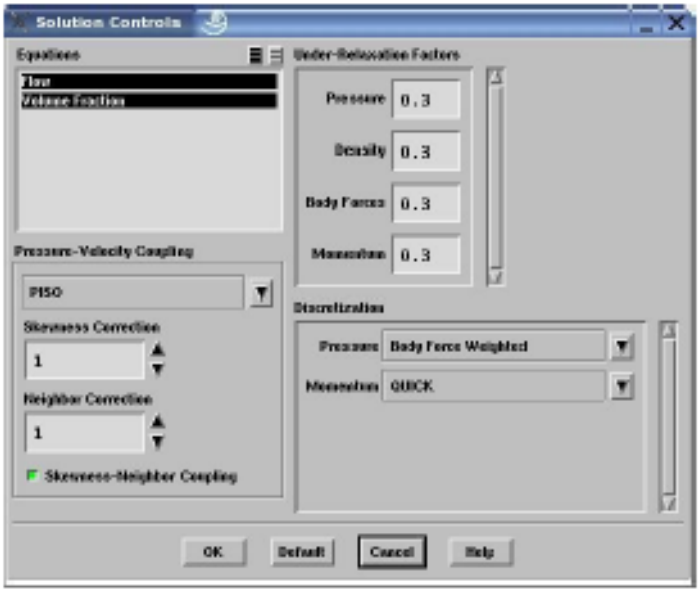

FIGURE 3- Solution Controls Window

21. Residual values for the equation of continuity and the equations of motion were set to 0.0001 (under the "Monitor Residual" command window). This value was chosen as a result of trial and error; a residual value of 0.0001 was the highest value that provided a comparatively fast convergence time.
22. FLUENT solved unsteady state problems based on a given time step. As seen in Figure 4, this was done using the Iterate command window. At large time step values, FLUENT solutions often do not converge. Therefore, a "Time Step" of 0.001 was chosen.

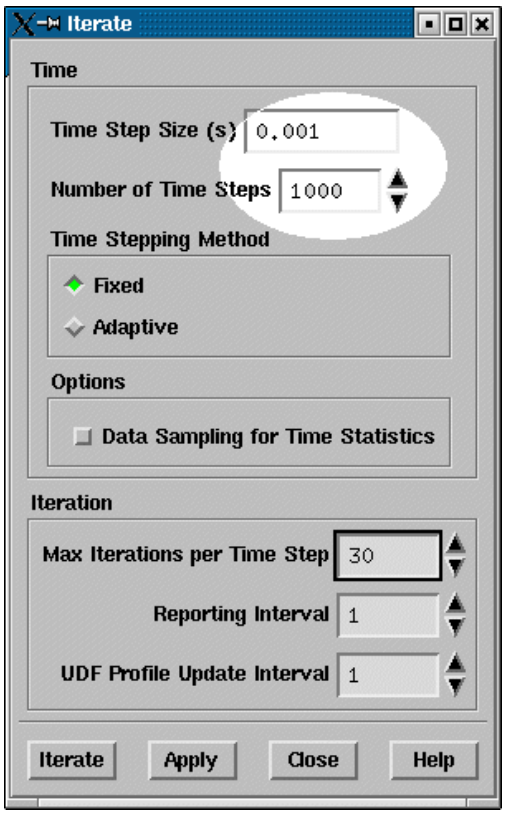

FIGURE 4 – Iterate Window

23. The FLUENT cases run were set to "Autosave", allowing review of the data at several different time steps. The orbital velocity was converted to seconds/revolution from radians/second. For each revolution 16 save points were taken and the number of time steps was chosen for Autosave Frequency.
24. The initial case and data files were saved using unique filenames that described which case was being run.

3. Running Cases in Batch Mode

Batch mode refers to the running of FLUENT files on Adelie supercomputer nodes. Submitting a file to a node allowed for a much faster runtime, with the one drawback being the lack of ability to view FLUENT while it was running. This

drawback was the reason that several autosave points are chosen. A batch file and an input file (Appendix C) were used to submit a FLUENT file to a dedicated node.

1. The batch file opened FLUENT and ran the case on an available node. The only amendment for different batch files was the input and output directories of the FLUENT file. Each batch file was saved using a name that ensured its compatibility with the associated case.
2. With FLUENT opened via the batch file, the input file read the initial case and data files, the number of time steps, the number of iterations per time step, and the final case and data files. All of these values were input and the batch file was saved according to the filename given to the batch file.

4. Obtaining Post-Processing Data in FLUENT

1. Once a FLUENT case was completed, several different items were investigated. Of most importance to the research were the wave shape and the shear stress on the bottom wall of the cylinder. Under the Contours menu, views of the contours were selected.
2. In order to view phase contours in the determination of phase transitions, "two" was selected in the Level Selection in the "Contours of Phases" menu. In order to see the wave shape, the cylinder was rotated by using the mouse.
3. Shear stress was investigated via the Contours menu. The number of levels was set to 100. In the "Contours Of" menu, Wall Shear Stress was selected.
4. To obtain plots of tangential versus radial shear stress across the cylinder bottom, x-wall shear stress and y-wall shear stress data were examined. The value in the

Camera window was changed to the “Bottom” view to observe the shear stress on the bottom of the cylinder.

5. Determining shear at a given point was done by “probing” with one of the mouse buttons on the desired point on the cylinder.
6. A hardcopy of the cylinder was saved to see shear distribution or the fluid wave. This was completed by using the “Graphics Hardcopy” command. The “PNG” was selected “PNG” as the format to ensure that a color image was captured.

IV. RESULTS AND DISCUSSION

A. Analysis of Steady State Behavior

As the dish motion starts up, flow patterns evolve (i.e., maximum fluid height, position of the fluid's leading edge). Initially, the maximum shear magnitude on the bottom of the dish will fluctuate. This is due to the fluid undergoing the rapid change from stagnation to high speed rotation. After a certain amount of time, the rotating fluid will reach a state where the maximum shear stress on the bottom of the dish either remains constant or fluctuates only slightly. When this condition is reached, the system is considered to be at steady state.

Three different cases were studied to determine an average time to reach steady state (dimensionless parameters corresponding to each case are shown in Table I). These cases correspond to certain dish and fluid properties (Appendix A). Each rotation point under study was equivalent to 0.1 seconds of dish rotation. In order to determine the maximum shear stress on the bottom of the dish, the phase contours were activated in FLUENT and maximum shear stress was selected. The camera view was set to bottom in order to properly orient the dish. Several points on the bottom of the dish nearest to the area of highest shear (as evidenced by a dark red contour) were probed (Figure 5) and the shear values averaged. These maximum shear stress values were graphed on an XY scatter plot with time on the X-axis and maximum shear (given in dyne/cm^2) on the Y-axis (Figure 6). Steady state was assumed when the maximum shear did not change by more than 0.1% between each time step. Once steady state was achieved the total time required was multiplied by the dish' orbital speed to determine the total number of orbits the dish has traversed.

TABLE I

DIMENSIONLESS PARAMETERS FOR STEADY STATE CASES

	Case A	Case B	Case C
Stokes Number	5	5	5
Froude Number	1.2	0.4	1
Slope Ratio	1	1	0.5

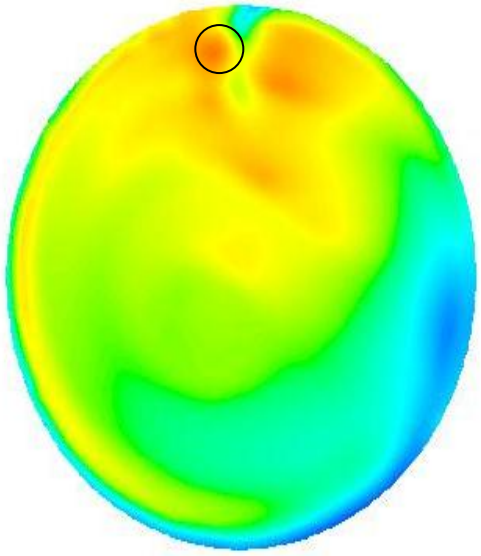

FIGURE 5 – Area of Maximum Shear Contour

For the three cases under study, the steady state was reached in one second for Cases B and C and all cases in 1.5 seconds (Figure 6). All cases had an orbital speed of 14.3 radians/second, indicating that steady state was achieved in four complete orbits of the dish.

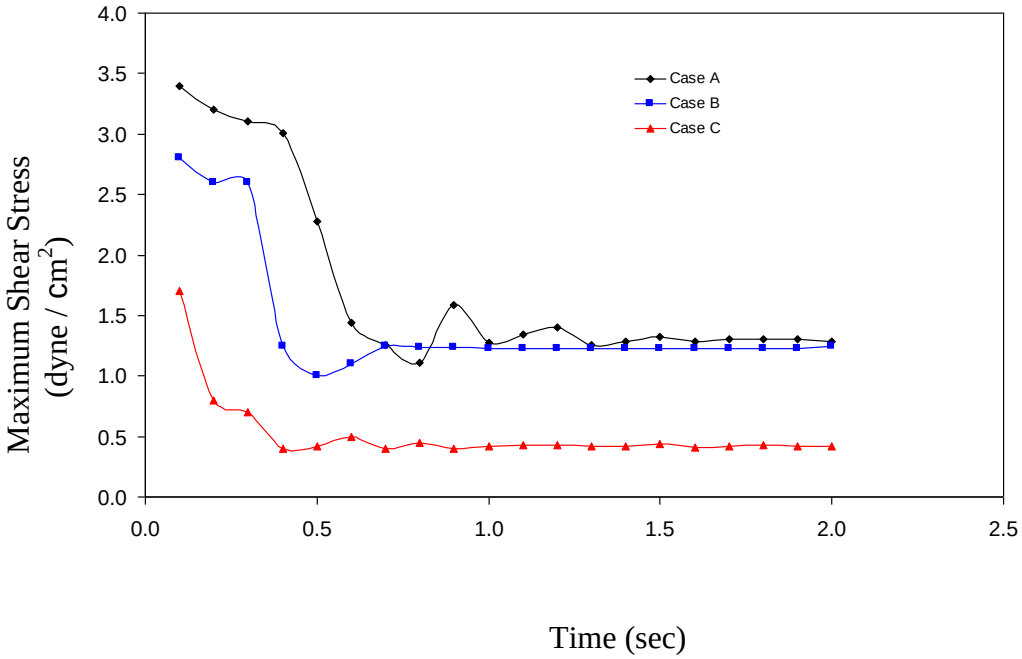

FIGURE 6 – Time to Reach Steady State for Cases A, B, and C

B. Analysis of Shear Stress Obtained via CFD

1. Determining Maximum Shear in an Orbiting Dish

For an orbiting dish model, the area of maximum shear stress has been shown to be on the bottom wall of the dish. Quantification of the maximum shear presents a challenge due to varying physical position of the fluid within the dish (Figure 7). The rightmost image in Figure 7 shows a phase of zero and increases with each counter-clockwise image until a full dish rotation is completed. A simplified point function provided by Ley et al. (1989) and utilized by many others [(Dardik, 2005), for example] does not take into account fluid height, a paramount variable for the calculation of shear stress for some flow conditions.

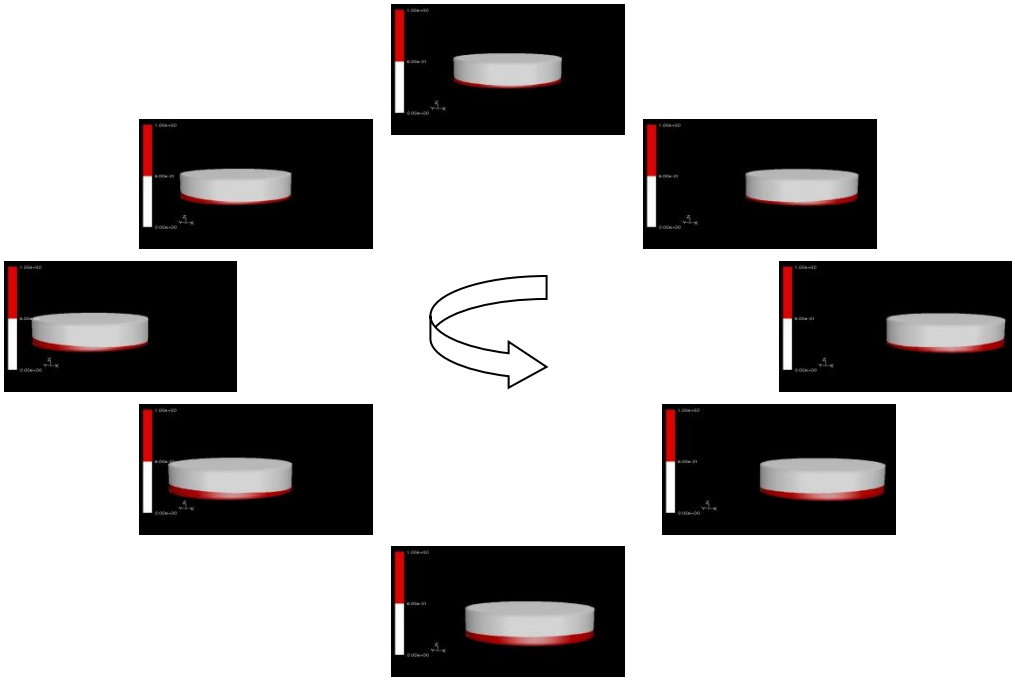

FIGURE 7 – Varying Fluid Position During Dish Rotation

Utilizing the CFD package FLUENT, physical parameters of cases run by Ley et al. (1989) were replicated and maximum shear values obtained. For each case, the area of maximum shear stress was determined by analyzing the shear contours. The phase and shear contours of a fluid of Stokes Number = 5 were compared. Shear contours are shown for the three dimensional view of the dish. It is evident that there are localized areas of maximum shear stress (Figure 9) both on the wall of the dish and on the bottom of the dish. The area of maximum shear stress on the bottom of the dish has a correlation with the trailing end of the fluid wave while the high shear area on the wall of the dish is in line with the peak of the fluid wave (Figure 8). Also evident is that the shear stress is not uniform thus showing that using a simplified point equation to determine the magnitude of wall shear stress does not completely describe the shear characteristics. The point function may be used for flow that satisfies Stokes' second problem of

oscillatory flow (low Reynolds number, low Froude number, low slope ratio and high Stokes number). Stokes' second problem specifically describes fluid oscillating on a thin boundary layer over a plate of infinite length. The oscillatory flow in an orbital dish has a finite length and side walls that add complexities to the fluid flow.

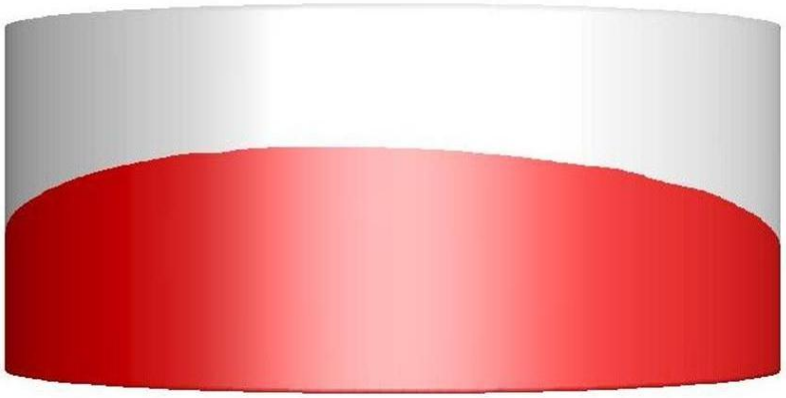

FIGURE 8 – Phase Contour of Stokes Number 5

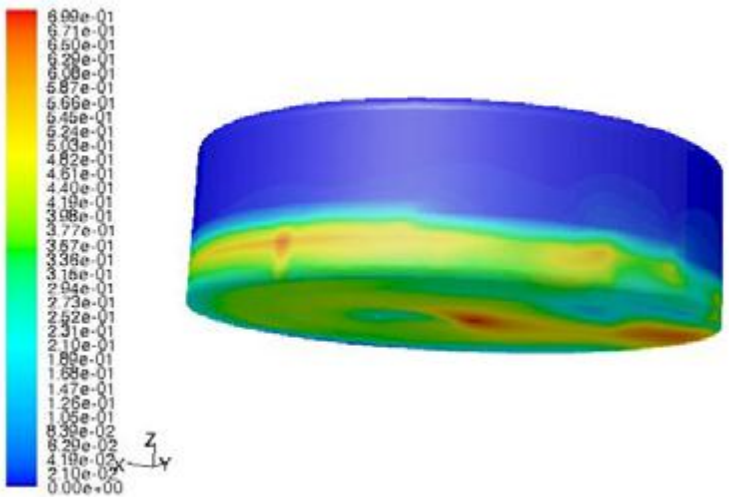

FIGURE 9 – 3-D Shear Stress Contour of Stokes Number 5

2. Comparison of Methods to Obtain Maximum Shear Stress

In order to demonstrate the differences in methods for determining the magnitude of maximum shear stress in an orbiting dish, two cases (D & E) were investigated (Table II). In both cases the formula posited by Ley et al. (1989) was used to calculate the magnitude of shear stress. These cases were also run in FLUENT and the magnitude of shear was observed on the shear contour in the center of the dish. The center of the dish was chosen so that any wall effects on shear magnitude were minimized. For further comparison the average value of shear stress was determined by overlaying a grid on the FLUENT shear contour (Figure 10), defining shear values at each point on the grid and averaging these values. Table III provides a summary of these shear data. These low shear stress values (<4 dyne/cm^2) were shown by Malek et al. (1999) to promote the formation of plaque on arterial walls and thus promote atherosclerosis. As the data show there are vast discrepancies in the results. As previously mentioned, Ley's equation fails to account for differences in the fluid height when the slope increases and subsequently increases wall effects; this omission is seen when the data are compared.

TABLE II

DIMENSIONLESS PARAMETERS FOR MAXIMUM SHEAR STRESS COMPARISON

	Case D	Case E
Stokes Number	2	2.5
Froude Number	0.7	0.8
Slope Ratio	0.4	0.3
Reynolds Number	100	100

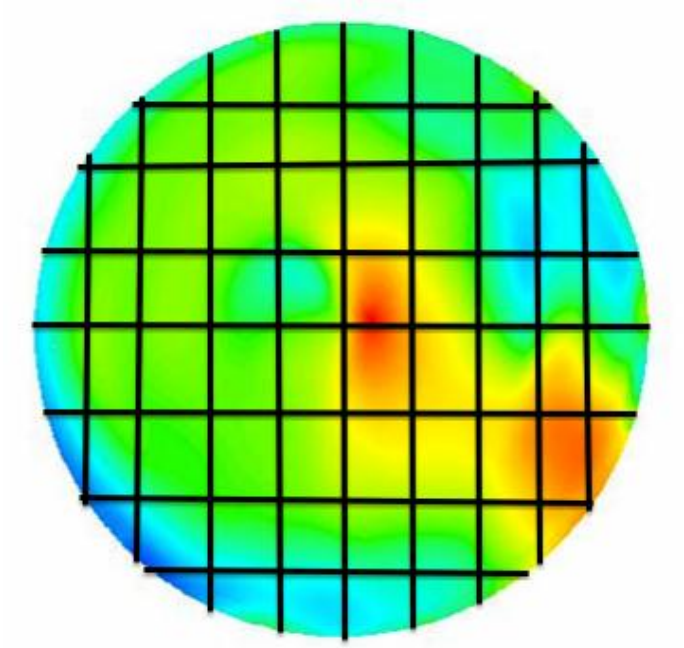

FIGURE 10 – Grid Overlay for Determining Average Shear of Case D

TABLE III

SHEAR STRESS COMPARISON

Method for Shear Determination	Case D	Case E
Ley's Equation	2.76dyne/cm^2	3.12dyne/cm^2
FLUENT (center)	0.67dyne/cm^2	1.11dyne/cm^2
FLUENT (average)	0.39dyne/cm^2	0.85dyne/cm^2

The equation used by Ley assumes a single steady shear stress. Cases D and E were further studied along ten points spanning the radius of the dish bottom (Figure 11). Shear values obtained from FLUENT were determined at each point. As Figure 12

shows, the shear is not steady at all. For both cases, the shear clearly changed across the radius.

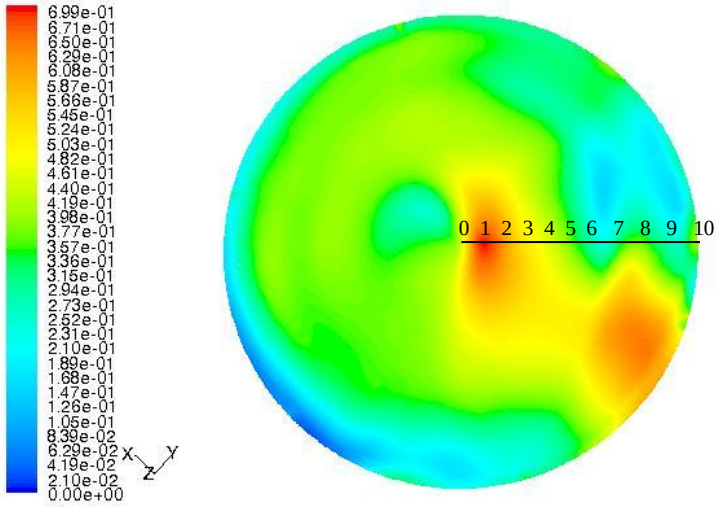

FIGURE 11 – Shear Determination of Case D at Varying Radii

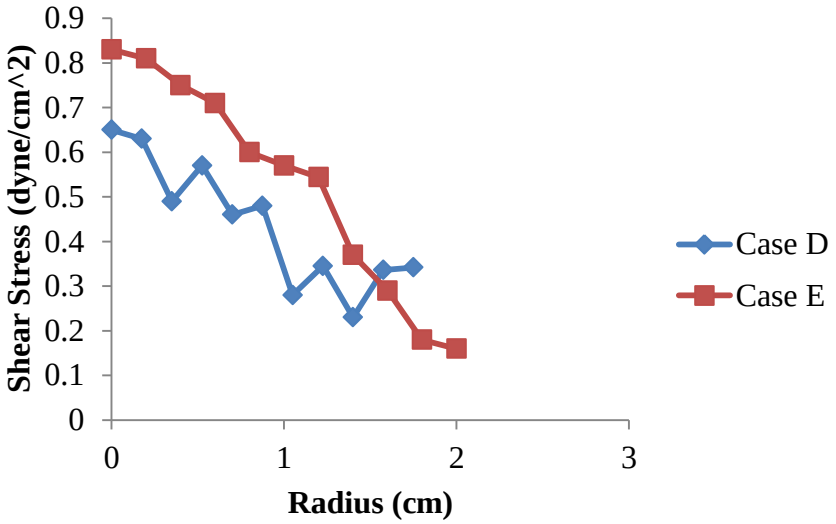

FIGURE 12 – Shear Variation across Radius

In a separate examination of the unsteady nature of shear across the bottom wall of an orbiting dish, the shear for Cases D and E were determined at 16 points around the dish at the same radius (Figure 13).

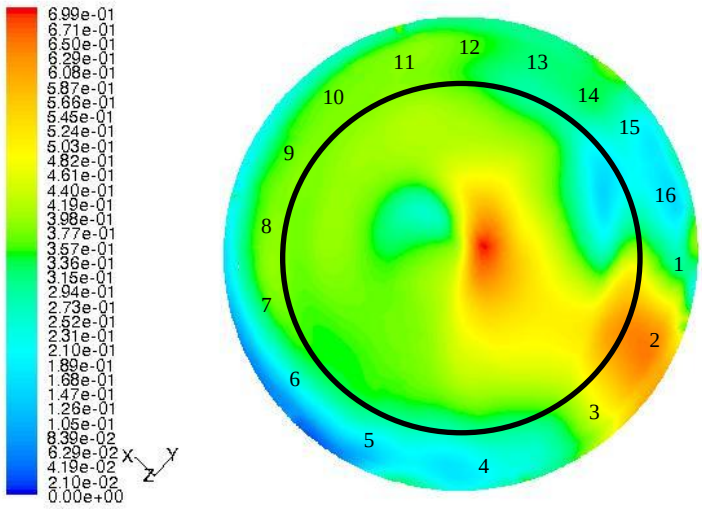

FIGURE 13 – Shear Determination of Case D at Same Radius

Figure 14 further illustrates the unsteady nature of shear stress on the wall of an orbiting dish. Even at the same radius around an orbiting dish the shear exhibited different values through each orbit. Case D gradually increased in shear until a maximum point then began to wane. Case E reached maximum then gradually decreased at the points around the same radius.

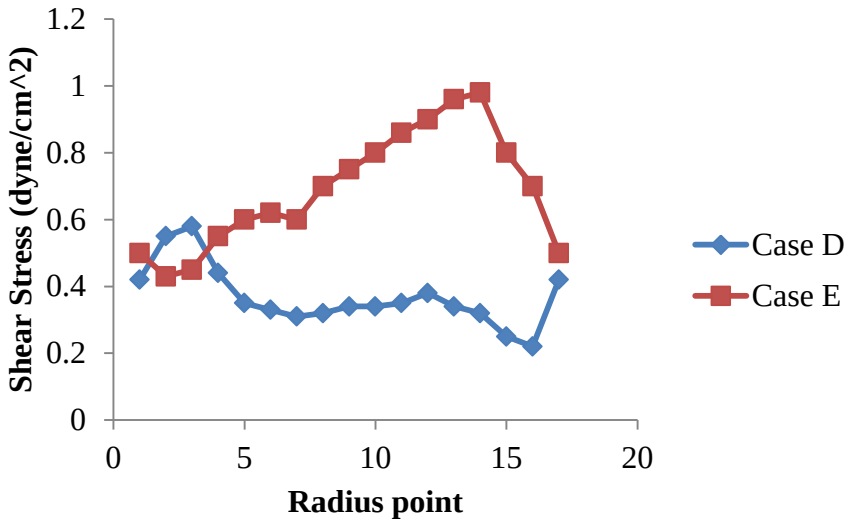

FIGURE 14 – Shear Variation around Orbiting Dish at Same Radius

C. Determination of Low Resolution Transitions for Dimensionless Parameters

When studying fluid flow in an orbital dish it is important to understand the various dimensionless parameters and what their respective effects are on the shear characteristics. Depending on the dimensionless parameter being investigated, the fluid will exhibit certain characteristics until the value of the parameter increases to a transition point. At this transition point the fluid will begin to exhibit different characteristics. In the most classic example of a fluid flowing through a pipe, a Reynolds number below 2300 is considered laminar flow and the fluid acts in a more steady fashion. When the Reynolds number rises above 4000 the fluid is in turbulent flow, characterized by a very unsteady flow full of eddies and vortices. In open channel flow the transition range is between 500 and 2000. By studying the effects of changing one dimensionless parameter at a time in FLUENT, transition points can be inferred for these low resolution cases. In order to show the same angle and fluid position on the surface, all fluid/dish contours (the

white contour being air and the red contour being liquid) are in the “Left” orientation where the x-axis is the horizontal plane and the z-axis forms the vertical plane. Shear contours are all viewed from the “bottom” orientation looking at the bottom of the dish.

1. Stokes Transition

As the Stokes Number increases, a lag is noticed with regards to the position of the fluid peak. Determination of this lag was done by overlaying a grid onto the fluid/dish contour and calculating the difference between the fluid peak and the center of the “left” view (Figure 15). Each gridline is a fraction of the total number of gridlines and 360 degrees.

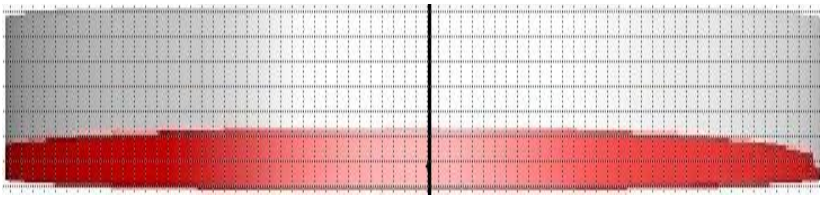

FIGURE 15 – Grid Overlay on the Fluid/Dish Interface

Fluid/dish interfaces are shown in Figure 16 for three separate Stokes Numbers with Froude Number constant at 1 and Slope Ratio constant at 1. The Stokes Number 2 interface shows the peak of the wave in line with the center of the orientation. This is indicative of zero degree phase lag and that any Stokes Numbers less than or equal to two are below the transition point. The interface at Stokes Number 10 shows a large lag in fluid peak. When the grid is overlaid, it was found that the peak actually lags 65 degrees. It may be inferred that any Stokes Number greater than or equal to 10 is above the transition point and that the actual transition point lies between Stokes Numbers of 2 and

10. At Stokes Number 5, the lag in the fluid peak slightly began to be seen at low resolution, with a calculated lag of 8 degrees. Intermediate values between Stokes Numbers of 2 and 5 were indeterminate as to any lag. This suggests that the transition range for Stokes Number with constant Froude Number and Slope Ratio is between 2 and 5.

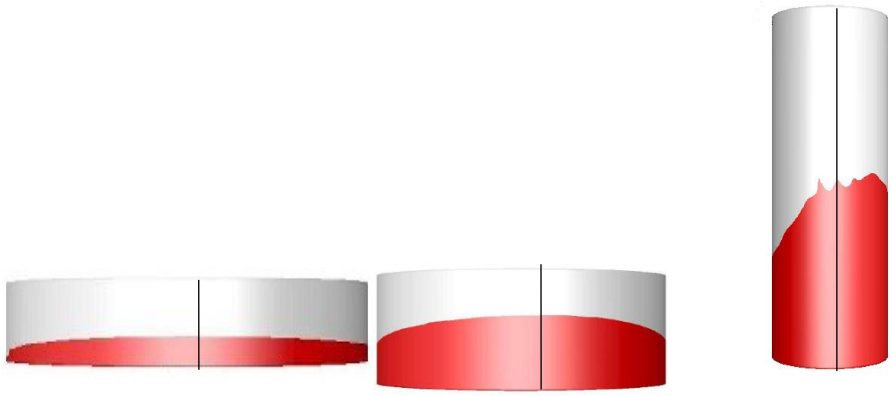

FIGURE 16 – Fluid/Dish Interface at Stokes Numbers 2, 5 and 10

Figure 17 shows the shear contours for the three Stokes Number cases under investigation. The wave is circulating counter-clockwise and is shown in the "bottom" orientation. At a Stokes Number of 2 the maximum shear stress was located in a small region with lower shear radiating from there. This region is the shallow area directly adjacent to the wave peak. As the Stokes Number increased to 5 and the beginning of transition, the maximum shear stress was less defined and emanated less smoothly with a more pronounced high shear zone. With the transition fully evidenced at Stokes Number 10, the shear stress was in a higher zone for more than half of the dish bottom.

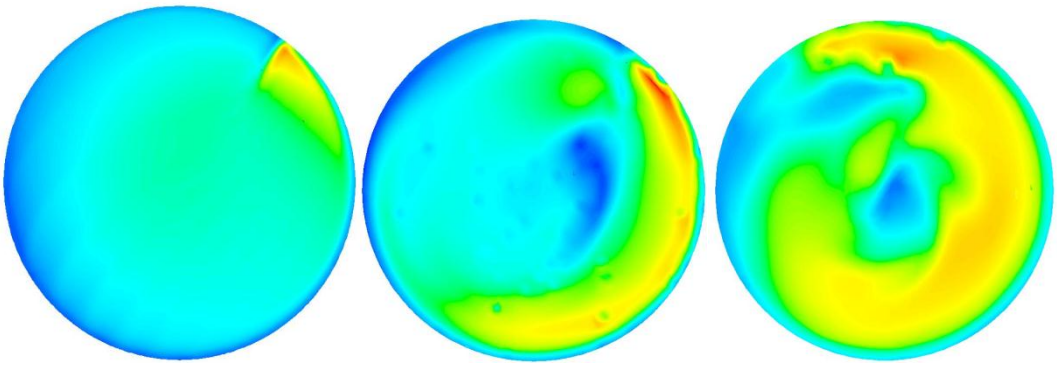

FIGURE 17 – Shear Contours at Stokes Numbers 2, 5 and 10

2. Froude Transition

The Froude Number is dependent upon the inertial forces of a fluid against gravitational effects. It is the magnitude of this "push and pull" ratio that causes a transition point, as evident when fluid in a dish begins to show a steepening of the leading edge of the circulating wave. Fluids with three separate Froude Numbers, holding Stokes Number constant at 5 and Slope Ratio constant at 1, are shown in Figure 18. At a Froude Number of 0.1 there was still continuity between fluid at the bottom of the dish and the trailing edge of the fluid. This indicated the Froude Number transition point being greater than 0.1 for fluid in an orbiting dish. A pronounced drop-off with a gap between the trailing edge and the bottom of the dish was seen at Froude Number 0.4 indicating that the fluid transition zone had been surpassed. The pronounced drop-off of the trailing edge was also seen for Froude Number of 0.2 with the exception that there was still continuity with regards to the trailing edge and the bottom of the fluid. Similar results were seen for Froude Numbers between 0.2 and 0.4 at low resolution, signifying

these values were the transition zone for Froude Number at these values of constant Stokes Number and Slope Ratio.

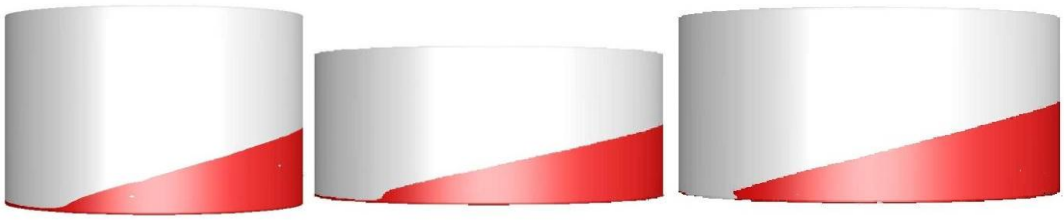

FIGURE 18 – Fluid/Dish Interface at Froude Numbers 0.1, 0.2 and 0.4

An examination of the shear contours for the three Froude Numbers investigated is seen in Figure 19. At the pre-transition Froude Number of 0.1, shear stress was mostly constant with only a small gap beginning to form in the two marked areas of highest shear. This gap became more pronounced as Froude Number was increased to 0.2 with higher values of maximum shear. The gap showed a separation beginning to develop and confirmed that this Froude Number would be part of a transition zone. For Froude Number 0.4 the gap was clearly defined as was seen with the fluid/dish interface for the same Froude Number and a transition was reached.

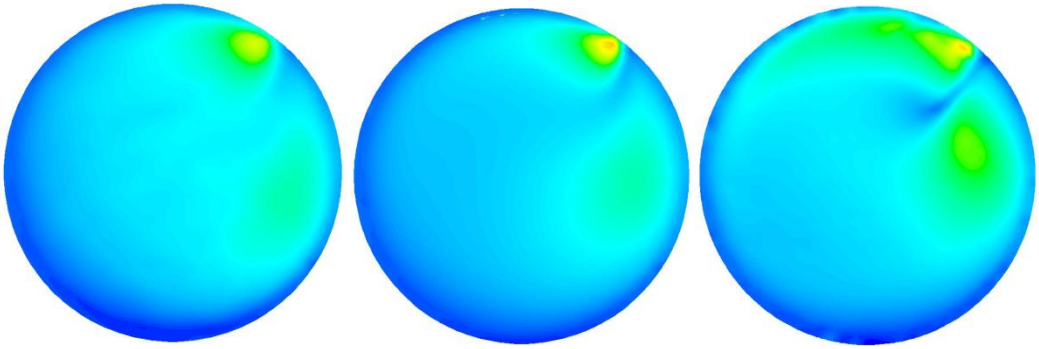

FIGURE 19 – Shear Contours at Froude Numbers 0.1, 0.2 and 0.4

3. Slope Ratio Transition

When the slope ratio reaches a transition point, the fluid peak will be high enough to create a dry area on the bottom of the dish. Figure 20 shows three different Slope Ratios while maintaining a constant Stokes Number of 5 and a constant Froude number of 1. At a Slope Ratio of 0.5 the fluid is still well defined as having both a peak and a bottom completely covered by fluid. This would indicate that the transition is greater than 0.5 Slope Ratio. For a Slope Ratio of 2 it is apparent that the height of the fluid peak has created not only a dry spot on the bottom of the dish but also an area of sharp transition. The transition zone occurs between 0.5 and 2. At Slope Ratio 1 the fluid still covers the bottom of the dish completely. For the low resolution FLUENT cases the dry area could only be seen at Slope Ratio 2. A higher resolution case would allow for a clearer, more quantitative indication of the actual transition.

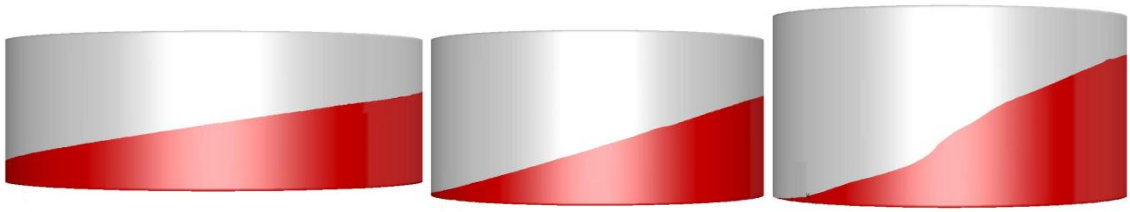

FIGURE 20 – Fluid/Dish Interface at Slope Ratio 0.5, 1 and 2

Shear contours for the three Slope Ratio values being investigated are seen in Figure 21. At the pre-transition Slope Ratio of 0.5, shear stress values > 0 were apparent across the entire wall. This is due to the presence of fluid across the entirety of the dish bottom. At the low end of the transition zone at Slope Ratio 1 a faint area of zero shear (dark blue) began to appear. This is an area where minimal fluid resides thus minimal shear is seen. For Slope Ratio of 2 the area of zero shear was more prominent, indicative of an area with no fluid.

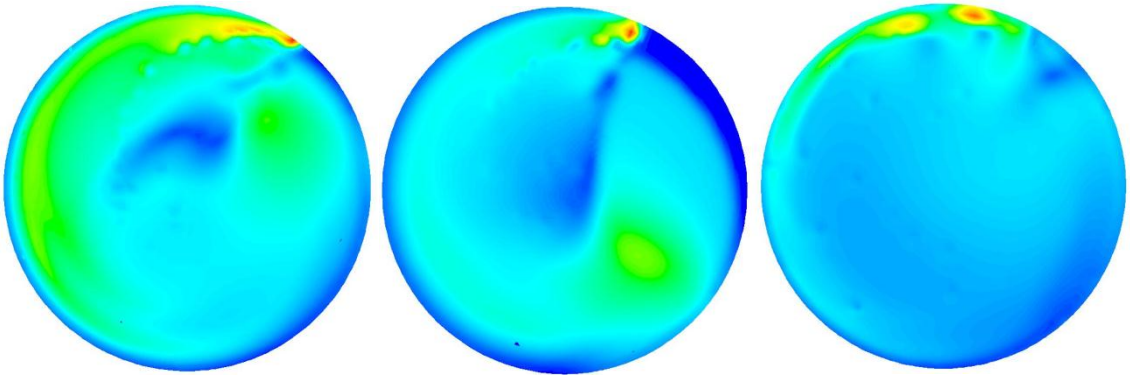

FIGURE 21 – Shear Contours at Slope Ratio 0.5, 1 and 2

V. CONCLUSIONS

- When studying the motion of fluid in an orbiting dish using computational fluid dynamics, a steady state is reached after the fluid rotates for 1.5 seconds at a low grid resolution. This correlates to four complete orbits of the dish.
- Using a simplified constant function to determine shear stress is inadequate to comprehensively describe shear characteristics on the bottom of an orbiting dish. The flow conditions present in an orbiting dish do not always conform to those of Stokes second problem, which does not take into account wall effects.
- A Stokes Number transition occurs as evidenced by a lag in the location of the fluid peak relative to the location of the dish.
- A Froude Number transition occurs as evidenced by a steep leading edge of the wave in the fluid.
- A Slope Ratio transition occurs as evidenced by a dry area forming on the bottom of the dish.
- CFD can be used to observe transitions of dimensionless parameters while maintaining constant values of other parameters.

VI. RECOMMENDATIONS

Further investigation of higher grid resolution CFD cases would provide a clearer, quantitative determination of transitions for Stokes number, Froude number, and slope ratio. Higher resolution cases would provide more accurate values of shear stress.

In order to confirm the data obtained using CFD, particle image velocimetry (PIV) experiments should be utilized to verify computational results.

REFERENCES

Alshihabi, S. N., Chang, Y. S., Frangos, J.A. and Tarbell, J. M. 1996. Shear stress-induced release of PGE_2 and PGI_2 by vascular smooth muscle cells. Biochemical and Biophysical Research Communications 224:808-814.

Banerjee, R. K., Back, M. R., Back, L. H. and Cho, Y. I. 2000. Physiological flow simulation in residual human stenoses after coronary angioplasty. Journal of Biomechanical Engineering 122:310-320.

Basombrio, F. G., Daria, E. A., Buscagliaa, G. C. and Feijoo, R. A. 2002. Numerical Experiments in Complex Hemodynamic Flows. International Journal of Computational Fluid Dynamics 16:231–246.

Belmonte, A., Eisenberg, H. and Moses, E. 1998. From Flutter to Tumble: Inertial Drag and Froude Similarity in Falling Paper. Physics Review Letters 81:345–348.

Berson R.E., Purcell M.R. and Sharp M.K., "Fluid motion in an orbiting culture dish," World Congress of Biomechanics, Munich, Germany, Jul 30 – Aug 4, 2006.

Bird, R. B., Stewart, W. E. and Lightfoot, E. N. 2002. Transport Phenomena. New York: John Wiley & Sons.

Crowe, C. T., Tsuji, Y., Sommerfeld, M. and Tsujinaka, Y. 1998. Multiphase Flows With Droplets and Particles. Boca Raton, FL: CRC Press.

Cunningham, K.S. and Gotlieb, A. I. 2005. The role of shear stress in the pathogenesis of atherosclerosis. Laboratory Investigation. 85:9-23

Dardik, A., Chen, L., Frattini, J., Asada, H., Aziz, F., Kudo, F. A. and Sumpio, B. E. 2005. Differential effects of orbital and laminar shear stress on endothelial cells. Journal of Vascular Surgery 41:869-880.

Davies, P. F., Dewey, C. F., Bussolari, S. R., Gordon, E. J. and Gimbrone, M. A. 1984. Influence of hemodynamic forces on vascular endothelial function. Journal of Clinical Investigation 73:1121−1129.

Faltinstein, O. 2006. Hydrodynamics of High-Speed Vehicles. London: Cambridge University Press.

Fluent Inc., 1996. FLUENT User's Guide.

Frangos, J. A., McIntire, L. V. and Eskin, S. G. 1988. Shear stress induced stimulation of mammalian cell metabolism. Biotechnology and Bioengineering 32:1053-1060.

Goncharov, V. N., Betti, R., McCrory, R. L., Sorotokin, P. and Verdon, C. P. 1996. Self-consistent stability analysis of ablation fronts with large Froude numbers. Physics of Plasmas 3:1402-1414.

Gotlieb, A. I. and Silver, M. D. 2001. Cardiovascular Pathology. New York: Churchill-Livingstone.

Greenhill, N. S. and Stehbens, W. E. 1983. Scanning electron-microscopic study of experimentally induced intimal tears in rabbit arteries. Atherosclerosis 49:119-126.

Haha, M., Yamashita, A., Paszkowiak, J., Sumpio, B. E. and Dardik, A. 2003. Oscillatory shear stress increases smooth muscle cell proliferation and Akt phosphorylation. Journal of Vascular Surgery 37:1277-1284.

Kraiss, L. W., Alto, N. M., Dixon, D. A., McIntyre, T. M., Weyrich, A. S. and Zimmerman, G. A. 2003. Fluid flow regulates E-selectin protein levels in human endothelial cells by inhibiting translation. Journal of Vascular Surgery 37:161-168.

Ku, D.N., 1997. Blood flow in arteries. Annual Review of Fluid Mechanics: 399-434.

Malek, A. M., Alper, S. L. and Izumo, S. 1999. Hemodynamic shear stress and its role in atherosclerosis. Journal of the American Medical Association 282:2035-2042.

Marshall, I., Zhaob, S., Papathanasopouloua, P., Hoskinsa, P. and Xub, X. Y. 2004. MRI and CFD studies of pulsatile flow in healthy and stenosed carotid bifurcation models. Journal of Biomechanics 37:679-687.

McCabe, W. L., Smith, J. C. and Harriott, P. 2001. Unit Operations of Chemical Engineering. New York: McGraw-Hill.

Levesque, M. J. and Nerem, R. M. 1985. The elongation and orientation of cultured endothelial cells in response to shear stress. Journal of Biomechanical Engineering 107:341-347.

Ley, K., Lundgren, E., Berger, E. and Arfors, K. 1989. Shear-dependent inhibition of granulocyte adhesion to cultured endothelium by dextran sulfate. Blood 73:1324-1330

Papathanasopoulou, P., Zhao, S., Köhler, U., Robertson, M. B., Long, Q., Hoskins, P., Xu, X. Y. and Marshall, I. 2003. MRI measurement of time-resolved wall shear stress vectors in a carotid bifurcation model, and comparison with CFD predictions. Journal of Magnetic Resonance Imaging 17:153-162.

Pirumov, U. G. 1998. Numerical analysis of two-phase flow in gas-dynamic filter. Numerical Mathematics and Programming

Resnick, N., Yahav, H., and Shay-Salit, A. 2003. Fluid shear stress and the vascular endothelium: for better and for worse. Prog. Biophys. Mol. Biol. 81:177-199.

Satcher, R. L., Bussolari, S. R., Gimbrone, M. A. and Dewey, C. F. 1992. The distribution of fluid forces on model arterial endothelium using computational fluid dynamics. Journal of Biomechanical Engineering 114:309-316.

Schaffer, J. P., Sanders, T. H., Saxena, A., Warner, S. B. and Antolovich, S. D. 2002. The Science and Design of Engineering Materials. New York: McGraw-Hill.

Sterpetti, A. V., Cucina, A., Morena, A. R., DiDonna, S., D'Angelo, L. S., Cavalarro, A. and Stipa, S. 1993. Shear stress increases the release of interleukin-1 and interleukin-6 by aortic endothelial cells. Surgery 114:911-914.

Tolliver, D. L. 1988. Handbook of Contamination Control in Microelectronics: Principles, Applications and Technology. Norwich, NY: William Andrew Publishing.

Wentzel, J. J., Gijsen, F. J., Stergiopulos, N., Serruys, P. W., Slager, C. J. and Krams, R. 2003. Shear stress, vascular remodeling and neointimal formation. Journal of Biomechanics 36:681-688.

Weston, S. J., Wood. N. B., Tabor, G., Gosman, A. D. and Firmin, D. N. 1998. Combined MRI and CFD analysis of fully developed steady and pulsatile laminar flow through a bend. Journal of Magnetic Resonance Imaging 8:1158-71.

Zarins, C. K., Giddens, D. P., Bharadvaj, B. K., Sottiurai, V. S., Mabon, R. F. and Glagov, S. 1983. Carotid bifurcation atherosclerosis, quantitative correlation of plaque localization with flow velocity profiles and wall shear stress. Circulation Research 53:502–514.

APPENDIX A

Case Parameters

Case	gravity (m/s^2)	orbital radius (cm)	cylinder radius (cm)	mean fluid height (cm)	orbital speed (rad/s)	kinematic viscosity (m^2/s)
A	9.8	1.2	1.44	0.36	14.29	7.41E-06
B	9.8	1.2	0.48	0.12	14.29	8.23E-07
C	9.8	1.2	0.6	0.15	14.29	1.29E-06
D	9.8	1.2	1.75	0.2	6.28	9.04E-06
E	9.8	0.8	2.0	0.2	6.28	4.02E-06

APPENDIX B

FLUENT User-Defined Function Creating Oscillatory Motion

```
#include "udf.h"
DEFINE_CG_MOTION(rotor_motion, dt, cg_vel, cg_omega, time, dtime)
{
real w,angle;
real offset = 0.;
real radius = 0.012;
w = 14.29;
NV_S (cg_omega, =, 0.0);
NV_S (cg_vel, =, 0.0);
angle = w*time + offset;
cg_vel[0] = -radius * w * sin(angle);
cg_vel[1] = radius * w * cos(angle); }
```

APPENDIX C

Batch and Input Files for Running FLUENT Cases

1. FLUENT Batch File

```
#!/bin/bash
#PBS -q dualcore2
#PBS -l nodes=1:ppn=1
#PBS -m e
#PBS -M mrpurc02@louisville.edu
INPUT_FILE=/scr/mrpurc02/Cases/CaseA/inputfile_uss
OUTPUT_FILE=/scr/mrpurc02/Cases/CaseA/outputfile
DIM=3d
PROG="/apps/Fluent.Inc/bin/fluent "
PROGARGS="$DIM -g -i $INPUT_FILE"
echo Running on:
cat $PBS_NODEFILE
NPROCS=`wc -l < $PBS_NODEFILE`
echo This job uses $NPROCS processors
hostname
$PROG $PROGARGS > $OUTPUT_FILE 2>&1
```

2. FLUENT Input File

```
rc /scr/mrpurc02/Cases/CaseA /CaseA_1.cas
rd /scr/mrpurc02/Cases/CaseA /CaseA_1.dat
solve
d
736
46
wc /scr/mrpurc02/Cases/CaseA /CaseA_1A.cas
wd /scr/mrpurc02/Cases/CaseA /CaseA_1A.dat
quit
exit
yes
```